

Effect of surface roughness on erosion rates of pure copper coupons in pulsed vacuum arc system

Lakshminarayana Rao and Richard J Munz¹

Department of Chemical Engineering, McGill University, Montréal (Québec) H3A 2B2, Canada

E-mail: richard.munz@mcgill.ca

Received 7 July 2007, in final form 17 October 2007

Published 30 November 2007

Online at stacks.iop.org/JPhysD/40/7753

Abstract

Vacuum arc erosion measurements were performed on copper cathodes having different surface roughness and surface patterns in 10^{-5} Torr vacuum (1.3324 mPa), in an external magnetic field of 0.04 T. Different surface patterns and surface roughness were created by grit blasting with alumina grits (G-cathodes) and grinding with silicon carbide emery paper (E-cathodes). The erosion rates of these cathodes were obtained by measuring the weight loss of the electrode after igniting as many as 135 arc pulses, each of which was 500 μ s long at an arc current of 125 A. The erosion rates measured indicate that erosion rates decrease with decreasing roughness levels. Results obtained indicate that both surface roughness and surface patterns affect the erosion rate. Having patterns perpendicular to the direction of cathode spot movement gives lower erosion rates than having patterns parallel to arc movement. Isotropic surfaces give lower erosion rates than patterned surfaces at the same roughness.

1. Introduction

High power electrical systems use vacuum circuit breakers as their chief safety device. Under operation, these vacuum switches must be able to withstand currents ranging from a few amperes to several 100 kA of current between their contacts for over a few 100 μ s. This is achieved by a vacuum arc between these contacts. Erosion of contacts in these safety switches determines their life [1]. Erosion of these contacts has been a subject of study for the past 50 years and it is well known that the negative contact (cathode) erodes faster than the positive contact [2–4]. Researchers have shown that many factors such as geometry of the cathode, operating vacuum, inter electrode gap, plasma forming gas, surface chemistry and electrode microstructure meaning the grain size affect the nature and extent of cathode erosion [5–12]. It was observed in 1942 by Cobine and Gallagher [13] that surface irregularities, like scratches, affect cathode spot movement in vacuum arcs. Although many researchers

mention the effect of surface roughness [14–16] on the erosion of cathodes only a handful of systematic studies are available in the literature. Daalder [17], in his meticulous study of the effect of surface roughness on erosion of copper cathodes, only reports on the effect of roughness on the size and movement of the cathode spots formed and not the erosion rate itself. Daalder and Vos [18] have shown that the arc voltages have different values on cathodes of different roughness. Fu [19, 20], studying the effect of surface roughness in the presence of an external magnetic field (B field), has reported that the cathode spot retrograde arc velocity is a strong function of the direction of the surface roughness. She has reported that when the grinding is in the direction of the spot motion imposed by the external B field, the arc velocities are several times higher relative to a perpendicular ground surface. She has observed that the arc voltage on rough surfaces was higher than the smooth surfaces in the presence of an external B field. But again she did not report on any erosion rate measurement which is a chief parameter in calculating the life time of a contact in vacuum circuit breakers.

¹ Author to whom any correspondence should be addressed.

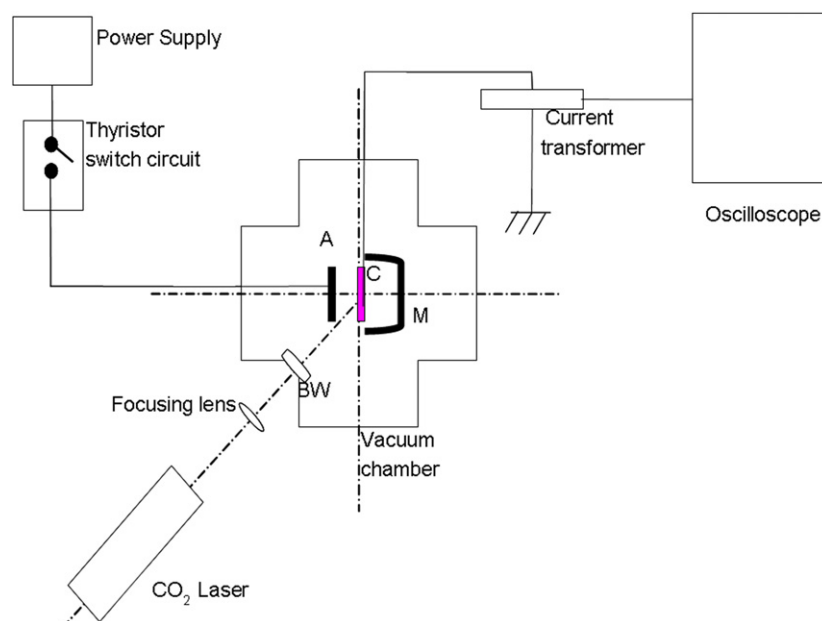


Figure 1. Schematic diagram of the experimental setup. A—anode; BW—beryllium window; C—cathode and M—permanent magnet. (This figure is in colour only in the electronic version)

In this paper, we report on the effect of surface roughness on the erosion rates of pure copper cathodes measured at 10^{-5} Torr vacuum (1.3324 mPa). Different surface roughness levels were created by grinding with three different sizes of silicon carbide emery papers and also by grit blasting the surface with two different sizes of alumina grits. Regular surface patterns were created by the emery method whereas grit blasting yielded isotropic rough surfaces. The different cathodes formed were characterized for their roughness levels using a surface profilometer and vacuum erosion rates on these cathodes were measured. Arc craters formed on these cathodes were analysed using a field effect scanning electron microscope (SEM) (Hitachi-4700). The results obtained were compared with the literature values of smooth pure Cu. The details are presented below.









2. Materials and experimental methods

Electronic grade oxygen free high electrical conductivity pure copper (99.99 wt%) was used in this study. As purchased machine finished copper bars were cut into rectangular strips of $60 \text{ mm} \times 12 \text{ mm} \times 3 \text{ mm}$ and used as cathodes for erosion experiments. Different surface patterns and surface roughnesses were created on these copper strips using two methods namely, grit blasting (further referred as G) and grinding with emery paper (further referred as E). Two different sizes of alumina grit, namely, $190 \mu\text{m}$ and $708 \mu\text{m}$, were blasted with nitrogen at 45 psig, to create an isotropic surface roughness and pattern. Three different sizes of silicon carbide emery paper, namely, $35 \mu\text{m}$ grit size, $95 \mu\text{m}$ and $190 \mu\text{m}$ grit size, were used to obtain a unidirectional surface pattern. Unidirectional surface patterns were created both parallel and perpendicular to the length of the copper strip. The surface roughness created was measured using a surface profilometer (DekTak) and the Ra values were calculated. Just before using

them for erosion studies these copper strips were carefully cleaned by ultrasound with acetone as the cleaning medium dried with a soft cloth and immediately installed into a vacuum chamber.

The schematic diagram of the experimental setup used for this study is shown in figure 1 and the details of the experimental setup are given elsewhere [21]. In essence, it consisted of a vacuum chamber, a power supply unit and a pulsed laser system. Vacuum chamber held the rectangular strip cathode mounted parallel to a rectangular Cu anode ($50 \text{ mm} \times 10 \text{ mm} \times 3 \text{ mm}$). Before the start of each experiment, the electrodes were placed in the chamber maintaining an inter-electrode gap of 5 mm and the chamber was pumped down to 10^{-2} Torr using a mechanical pump. At this vacuum, the reactor was filled with ultra high purity argon and then pumped to 10^{-5} Torr by a mechanical and an oil diffusion pump connected in series. A permanent U-shaped magnet (B field = 0.04 T) was positioned behind the cathode to move the cathode spots in the retrograde direction, parallel to the length of the copper strip. Capacitors in the arc power supply unit were charged to an open circuit voltage of 200 V. A pulsed arc was initiated on the cathode by a $1 \mu\text{s}$ pulse of $10.6 \mu\text{m}$ infrared laser radiation from a 1.2 kW Diamond™ K-500 CO₂ laser system, supplied by Coherent technologies. A thyristor based electrical switching circuit was used to control a $500 \mu\text{s}$ arc duration over which, a constant current of 125 A was maintained. This square current pulse was measured using an externally triggered HP-54503A digital oscilloscope. To determine the erosion rate, as many as 135 arc pulses, each $500 \mu\text{s}$ long with a current of 125 A, were run on the cathode. These pulses were run at a rate of 3–4 pulses per minute. The erosion rate values in grams per coulomb (g C^{-1}) were measured by weighing the cathode before and after the arcing, using a digital balance (accuracy $\pm 1 \times 10^{-4}$ g) and then dividing the weight difference by the total electric charge $Q = \int I dt$, passing through the cathode. For each surface pattern and

Table 1. Summary of the cathode studied ('-llei': parallel, '-ular': perpendicular).

Name	Preparation method	Grit size (μm)	Roughness Ra [μm]	Pattern type
E-36-llei	Grinding with emery	36	0.86 ± 0.1	 Parallel to sample length
E-36-ular	Grinding with emery	36	0.66 ± 0.1	 Perpendicular to sample length
E-95-llei	Grinding with emery	95	1.70 ± 0.1	 Parallel to sample length
E-95-ular	Grinding with emery	95	1.48 ± 0.1	 Perpendicular to sample length
E-190-llei	Grinding with emery	190	2.67 ± 0.3	 Parallel to sample length
E-190-ular	Grinding with emery	190	2.64 ± 0.1	 Perpendicular to sample length
G-190	Grit blasting	190	3.31 ± 0.1 (Direction parallel) 3.31 ± 0.1 (Direction perpendicular)	 Isotropic
G-708	Grit blasting	708	7.32 ± 0.1 (Direction parallel) 7.42 ± 0.1 (Direction perpendicular)	 Isotropic

roughness, erosion rates were measured on three individual cathodes. An average of these three measured values was calculated and reported as average erosion rate. To account for the loss of material due to the 1000 ns laser pulse, which was used to initiate the arc, the weight loss of the cathode was determined under identical experimental conditions, by imposing 135 laser pulses on the machine finished pure Cu with no arcs. This weight loss, which was $\sim 15\%$ of the total weight loss, was removed before calculating the erosion rates.

3. Results and discussion

3.1. Surface roughness characterization

The cathodes prepared were characterized for their roughness, Ra values, using a surface profilometer. Table 1 gives a summary of the surface patterns and the Ra values for each kind of cathode used. Each kind of cathode was scanned for a length of 0.5 cm in the soft touch mode and the Ra

values were computed with inbuilt software. Two individual measurements were made on each kind of cathode and the standard deviations computed are reported as error in table 1. On surfaces prepared by emery paper (E-cathodes), which had unidirectional patterns, the surface was only scanned perpendicular to the direction of the pattern created whereas on surfaces prepared by grit blasting (G-cathodes), surface was scanned in both parallel and perpendicular directions. We see that the Ra values increase with the grit size used. For G-cathodes, the Ra values were similar in both parallel and perpendicular directions showing that the roughness created was isotropic. On E-cathodes, at a particular emery grit size, both parallel patterned and perpendicular patterned cathodes had similar Ra values. Thus the only difference between the two kinds of E-cathodes prepared from the same emery paper is the surface pattern.

Figure 2 shows a plot of Ra versus grit size used. We see that the Ra value of E-190 cathodes is slightly lower than that of G-190 cathodes although the grit size used in both the cases were same.

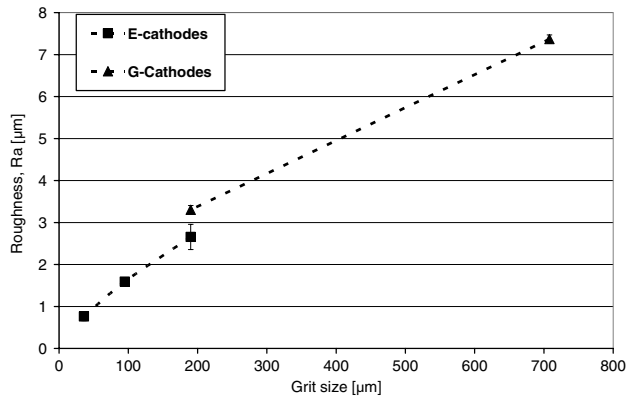


Figure 2. Roughness Ra versus grit size.

Figure 3 shows the SEM pictures for each kind of cathode used. For E-cathodes, only cathodes having parallel patterns are shown here since the SEM pictures of the surfaces with perpendicular patterns had similar features. Figures 3(a)–(c) are SEM pictures of E-cathodes prepared from grit size 36 μm , 95 μm and 190 μm , respectively. We can see the unidirectional ridges on the surface which are mostly parallel to each other. Individual ridges have many sharp projections. Comparing figure 3(a) with 3(c) we can clearly see that, as the grit size is increased, the width of the ridge formed is also increased and so is the separation between the individual ridges. Figures 3(d) and (e) are the SEM images of the G-cathode formed after grit blasting with 190 μm and 708 μm alumina grits, respectively. On these cathodes no directional features are noticeable, which corroborates the isotropic Ra values measured. The cathode formed from 708 μm grit has larger irregular features (shown by the dotted circle) when compared with the features observed on the cathodes formed from 190 μm alumina grits.

3.2. Cathode erosion rate

Table 2 summarizes the erosion rates reported in the literature for pure massive Cu. For arcs of 100–125 A, in 10^{-6} Torr vacuum, an erosion rate of the order of $100 \mu\text{g C}^{-1}$, is generally agreed upon [4]. In all the references cited in table 2, the authors do not report on any special surface roughness preparation or measurement and hence we consider that the cathodes tested had machine finished surfaces (formed after cold rolling).

Figure 4 shows the erosion rates and the Ra values measured on the cathodes tested in this study. The error bars reported in figure 4 are the standard deviations of the values obtained from three separate measurements.

In figure 4, for both E-cathodes and G-cathodes tested, we see that the erosion rate decreases with the Ra values. In the group of E-cathodes, E-36 μm cathodes have the lowest Ra value of $0.86 \mu\text{m}$ and also have the lowest erosion rate of $30 \mu\text{g C}^{-1}$. Similarly in the G-cathodes group, G-190 μm cathodes have the lowest Ra value of $3.30 \mu\text{m}$ and gave an erosion rate of $33 \mu\text{g C}^{-1}$.

Comparison between parallel and perpendicular patterns on E-cathodes. In figure 4, for any particular grit used, we see that the average erosion rate (average of three individual

measurements) of cathodes having perpendicular patterns is lower than the average erosion rate of cathodes with parallel patterns. Although, error bars for both E-95 μm cathodes and E-36 μm cathodes overlap, we clearly see that E-190-ular cathodes have an average erosion rate of $45 \mu\text{g C}^{-1}$ whereas E-190-llel cathodes have an erosion rate of $106 \mu\text{g C}^{-1}$. This trend can be explained by analysing the arc traces formed on these cathodes and is discussed in detail below.

Figure 5 shows the images of the arc trace left on the cathodes after 135 arc pulses. For all the cases, multiple arcs were initiated at different vertical positions on the cathode by moving it vertically. Once the arc was ignited, a permanent U-shaped magnet moved the arc down in the retrograde direction as shown by an arrow in figure 5. Figures 5(a) and (b) are an SEM image of the arc trace on E-190-ular surface and E-190-llel surface, respectively. From figure 5, we can clearly see that the arc trace formed on cathodes with perpendicular patterns is wider compared with the arc trace formed on cathodes with parallel pattern. The arc trace formed on parallel patterns is made up of individual arc traces either separate and/or overlapping on one another which are very narrow compared with their perpendicular pattern counterpart. From detailed analysis of the arc trace under an optical microscope, we noticed that, on both parallel and perpendicular patterned cathodes, the cathode spots clearly follow the surface patterns created. Similar to what we observe, researchers have reported earlier in the literature that the vacuum arcs tend to follow the surface scratches [1, 13–16, 19, 20]. That is, vacuum arcs which are composed of many individual current carrying micro/macro-attachment points (cathode spots), move by successive initiation and extinction of cathode spots. It is well documented that new cathode spots always initiate along a surface scratch, if present [13–16, 19, 20]. So, on E-cathodes with perpendicular patterns, the natural tendency of the arc is to move sideways on the cathode, but the B field created by the permanent magnet pushes the arc downwards. Due to the combined effect of these two, the arc attachment on the surface becomes wider, resulting in a wider arc trace relative to the arc trace formed on E-cathodes with parallel patterns. On E-cathodes with parallel patterns, the B field force is in the same direction as the surface pattern which also happens to be the natural direction of arc movement. Hence on E-cathodes with parallel patterns, the final arc trace is narrow.

Figure 6 shows the SEM pictures of the arc trace formed on E-190-ular pattern. Figure 6(a) through 6(d) shows the successive images increasing magnification of the arc craters formed (the magnified section is shown by a rectangle as we proceed from image to image). We can clearly see that the macro craters are only present along the scratches and that the regions between the ridges are free from arc craters. If one were to analyse the arc motion at the micro level, the arc once ignited on a surface with perpendicular patterns, would start on a particular ridge (say i th ridge) and tend to move sideways. That is, new cathode spots would be created one next to the other along the i th ridge. Now due to the B field force, the cathode spot would jump from the i th ridge to the $(i + 1)$ th ridge, which is right below the i th ridge, and then start to move sideways on this $(i + 1)$ th ridge. Further, it would

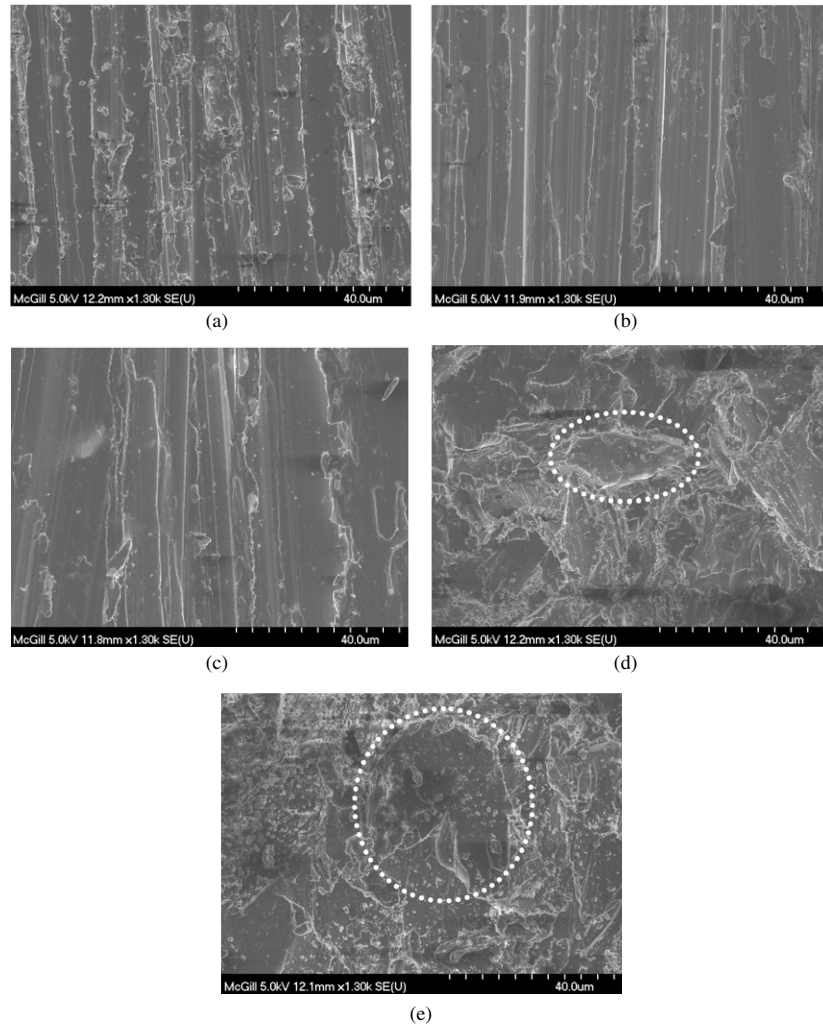


Figure 3. SEM images of the cathodes: (a) E-36-llel; (b) E-95-llel; (c) E-190-llel; (d) G-190 and (e) G-708. Dotted circle shows the individual features present on the cathode.

jump down again to $(i + 2)$ nd ridge and so on. If the above argument were true, then the SEM observations of the arc trace should reveal macro craters formed only along the ridges. The pictures presented in figure 6, support the above argument. Similar results were seen on both E-95-ular and E-36-ular cathodes.

Extending the above argument, if the average distance between the i th and $(i + 1)$ th ridge is increased, then the arc has to jump a larger vertical distance as it moves down the cathode. This should result in a higher residence time of the arc on the i th ridge before jumping onto the $(i + 1)$ th ridge. It is well documented in the literature that the erosion of cathodes is a heat transfer problem. Higher arc residence time on the cathode results in higher erosion rates [25]. As shown in figure 3, when we move from E-36-ular cathodes to E-190-ular cathodes, in addition to increasing the roughness level, we are also increasing the average separation between the unidirectional ridges formed. Thus, one would expect higher erosion rates on E-190-ular cathodes than on E-36-ular cathodes. The erosion rates results reported in figure 4 support this argument.

Figure 7 shows the SEM pictures of the arc trace formed on E-190-llel pattern. Figure 7(a) through 7(d) shows the

Table 2. Erosion rates of pure massive Cu reported in the literature.

Reference	Arc current (A)	Vacuum level (Torr)	Erosion rate ($\mu\text{g C}^{-1}$)
1 Plyutto <i>et al</i> [22]	120	1×10^{-6}	130
2 Kimblin <i>et al</i> [23]	80	1×10^{-6}	115
3 Boxman <i>et al</i> [4] (p 233–4)	125	1×10^{-5}	90
4 Meunier <i>et al</i> [24]	≤ 300	1×10^{-6}	70–80

successive images of the arc craters formed. We can clearly see from these images that the arc craters are lined up one below the other. Larger overlapping craters are clearly visible in figure 7(d). Due to the combined effect of increased local heating and formation of multiple arc craters one above the other, the E-190-llel cathode gives higher erosion rate in comparison with its counterpart E-190-ular. On E-190-ular cathodes, the arc craters are more distantly spaced other as is seen in figure 6 and this result in better heat dissipation on the cathode surface giving lower erosion rates. Analysing the arc motion on the cathodes with parallel patterns, the arc once ignited would move along a particular ridge and the cathode

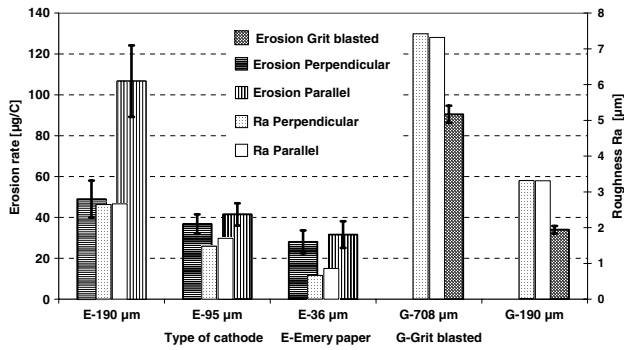


Figure 4. Erosion rate and roughness levels of cathodes prepared by emery paper and grit blasted cathodes.

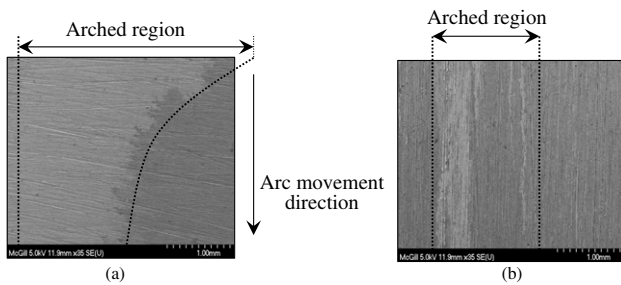


Figure 5. Arc trace formed on: (a) E-190-ular cathode; (b) E-190-llel cathode. The brighter region between the dotted lines is the arc trace. The solid arrow shows the direction of arc movement.

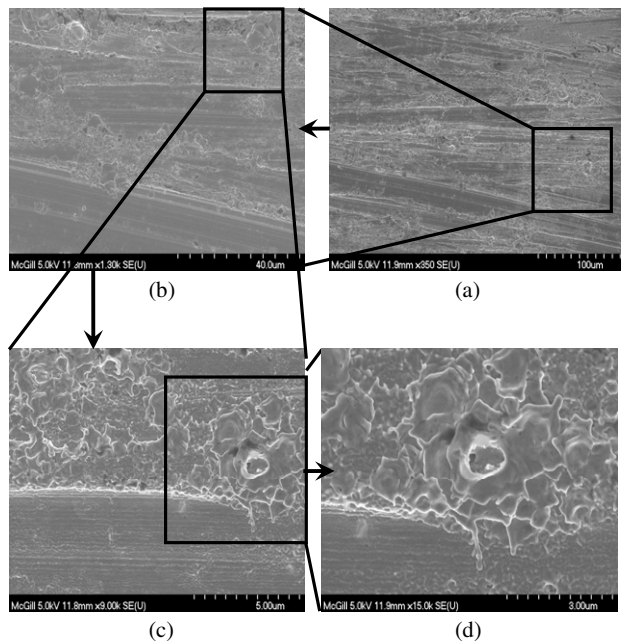


Figure 6. SEM images of the arc craters formed on E-190-ular cathode (magnification increases from (a) to (d)).

spots would line up one below the other. This should result in multiple overlapping craters and also result in increased local heating of the cathode. Pictures presented in figure 7, support this argument very well. Similar crater formations were observed on E-95-llel and E-36-llel cathodes.

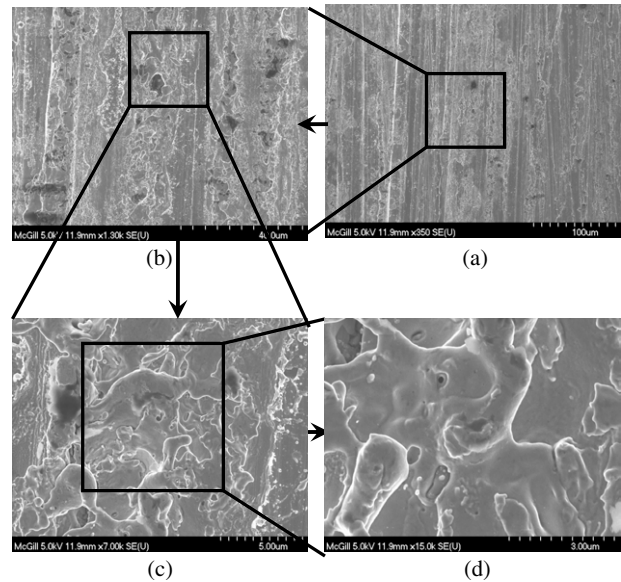


Figure 7. SEM images of the arc craters formed on E-190-llel cathode (magnification increases from (a)–(d)).

We notice from figure 4, between E-95 μm and E-36 μm cathodes, though there is a significant reduction in the roughness levels there only a slight reduction in the erosion rates. The erosion error bars on all these cathodes overlap showing a plateau effect in the erosion rate with roughness level. This result is attributed again to the nature of arc attachment and the surface patterns. If the dimensions of the surface pattern start to become comparable to the size of the macro craters formed, then the original surface roughness and pattern created would be destroyed in the first few passages of the arc. This would result in a constant roughness irrespective of the original roughness level/pattern. Figure 8 shows the SEM images on E-95-ular and E-36-llel cathodes. Here we can see that the arc craters formed have destroyed the initial pattern in spite of the fact that both the grit size used and pattern formed were different. Hence the overall erosion rate measured on these cathodes would be the same irrespective of their initial roughness level.

In pulsed vacuum arc experiments, arc velocity is generally calculated by dividing the length of the arc trace with the pulse duration [18–20]. Fu and Smeets [19, 20] working on similar studies as ours, observed higher arc velocities on cathodes having parallel patterns. Generally, higher arc velocities result in a lower residence time of the arc, and lower erosion rates. As shown in figure 4, the parallel patterned cathodes have higher erosion rates which are counterintuitive. Although the cathode spot velocities on the parallel patterned cathodes may be higher, the overall erosion rates are also higher due to the formation of over lapping craters and increased local heating.

Erosion rates on G-cathodes and comparison with E-cathodes. Figure 9 shows a plot of erosion rate versus grit size used. From figures 2 and 9, we can see that the erosion rates of G-cathodes also show a similar trend with roughness as E-cathodes. That is, the erosion rate increases with Ra. G-708 μm cathodes which have an Ra value of 7.32 μm give an erosion rate of

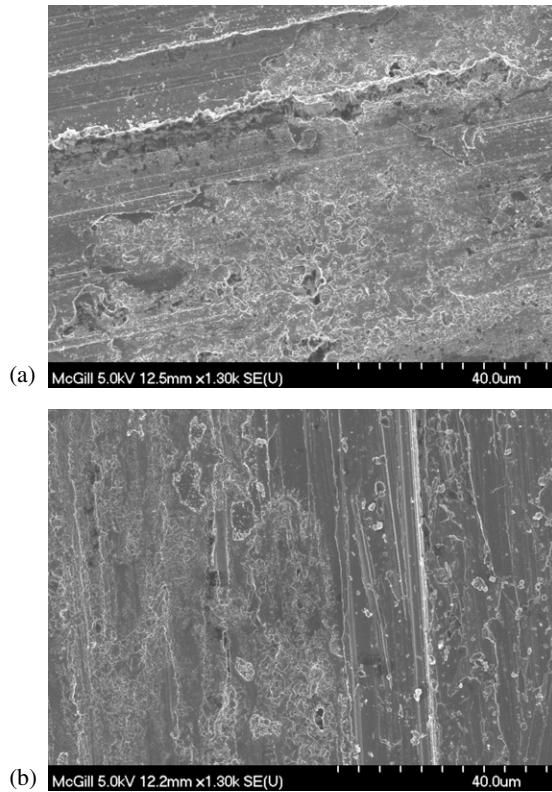


Figure 8. SEM images of arc trace formed on (a) E-95-ular cathode; (b) E-36-llel cathode.

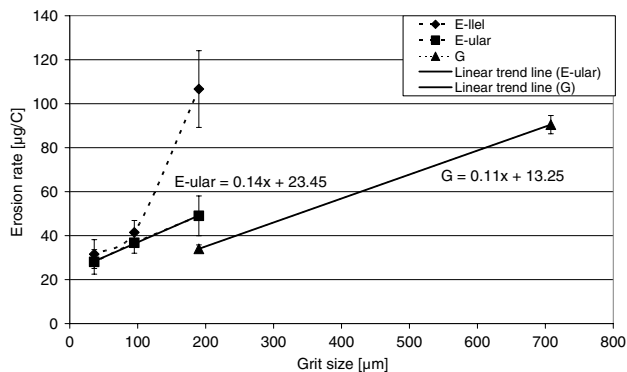


Figure 9. Erosion rate versus grit size. Linear trends (—) lines for E-ular and G-cathodes have similar slopes.

$90 \mu\text{g C}^{-1}$ whereas G-190 μm cathodes which have an Ra value of $3.31 \mu\text{m}$ give an erosion rate of $33 \mu\text{g C}^{-1}$. The reason for this trend is again explainable by the surface features present on the cathodes as shown in figures 3(d) and (e) G-708 μm cathodes having larger surface features give higher erosion rates when compared with G-190 μm cathodes which have smaller surface features.

From figure 2, we can see that the G-190 μm cathodes have Ra value of $3.31 \mu\text{m}$ which is slightly greater than the Ra value of $2.67 \mu\text{m}$ for E-190 μm cathodes. As shown in table 1, the grit size used to prepare both G-190 μm and E-190 μm cathodes was 190 μm . G-190 cathodes, which have an isotropic pattern give lower erosion rates when compared to E-190 cathodes which have a unidirectional pattern. We see from figure 4 that the average erosion rates of G-190 μm

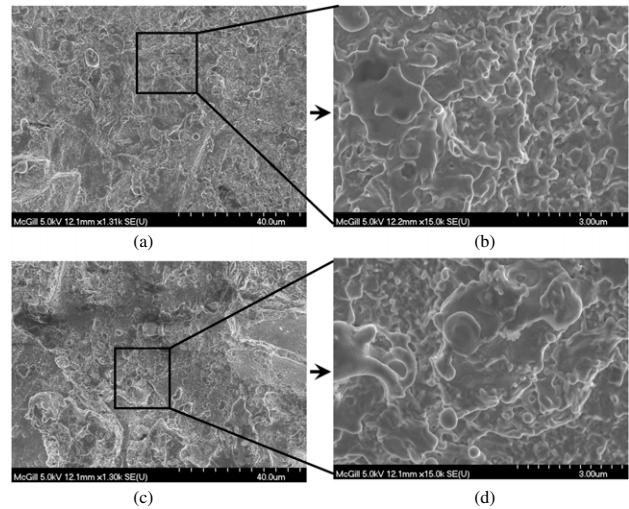


Figure 10. SEM images of the arc craters formed on: (a) and (b) E-190 cathodes; (c) and (d) G-708 cathodes.

cathodes is $33 \pm 2 \mu\text{g C}^{-1}$ whereas the average erosion rate of E-190-ular cathodes is $49 \pm 9 \mu\text{g C}^{-1}$. Also, we can see from the added trend lines, that the slopes for both E-ular and G-cathodes are similar. However, the erosion rates do not scale with the Ra values for E- and G-cathodes. G-708 μm cathodes which have the highest Ra value of $7.42 \mu\text{m}$ has an average erosion rate of $90 \mu\text{g C}^{-1}$ whereas E-190-llel cathodes which has on Ra value of $2.67 \mu\text{m}^{-1}$, also has average erosion rate of $108 \mu\text{g C}^{-1}$. The reason for this behaviour is not known at this point, but is probably due to the arc motion on isotropic roughness.

Figure 10 shows the SEM images of the arc craters formed on G-190 μm and G-708 μm cathodes. The arc craters formed on G-190 μm cathodes are smaller in dimension ($\sim 2 \mu\text{m}$) relative to the arc craters formed on G-708 μm cathodes ($\sim 3\text{--}4 \mu\text{m}$). Similar to earlier reports in the literature, formation of large craters is consistent with higher erosion rates [26].

4. Conclusions

We conclude that

- For both E- and G-cathodes tested, vacuum erosion rates reduce with reducing surface roughness levels.
- At higher roughness levels (Ra closer to $2.67 \mu\text{m}$) both surface roughness and surface patterns affect erosion rates. At higher roughness levels, having surface patterns perpendicular to the direction of arc motion results in lower erosion rates. Cathodes with perpendicular patterns give lower erosion rates due to wider arc attachment. This results in reduced local heating and better heat dissipation on the cathode surface. However, when the surface roughness levels are reduced (Ra lower than $1.48 \mu\text{m}$), the roughness levels and surface patterns do not seem to affect the erosion rates.
- Erosion rates depend mainly on the nature of arc attachment and arc movement on the cathode. At any roughness level, having regular patterns in the direction of arc movement, results in overlapping craters and higher erosion rates. Isotropic surfaces promote random motion and hence give lower erosion rates.

Acknowledgments

The authors express their gratitude to Dr Jean-Luc Meunier of McGill University, Chemical Engineering Department, Montreal, Canada, for valuable suggestions and discussions. The financial support of the Natural Sciences and Engineering Research Council of Canada for the work is gratefully acknowledged.

References

- [1] Daalder J E 1978 Cathode erosion of metal vapour arcs in vacuum *PhD Thesis* Eindhoven University of Technology, Netherlands
- [2] Boxman R L 1977 Twenty-five years of progress in vacuum arc research and utilization *IEEE Trans. Plasma Sci.* **25** 1174–86
- [3] Farrall G A 1980 Electrical breakdown in vacuum *Arcs: Theory and Application* ed J M Lafferty (New York: Wiley)
- [4] Boxman L R, Sanders D M and Martin P J 1995 *Handbook of Vacuum Arc Science and Technology: Fundamentals and Applications* (New Jersey: Noyes Publications)
- [5] Beilis I I 2001 State of the theory of vacuum arcs *IEEE Trans. Plasma Sci.* **29** 657–70
- [6] Schmoll R 1998 Analysis of the interaction of cathode micro protrusions with low-temperature plasmas *J. Phys. D: Appl. Phys.* **31** 1841–51
- [7] Farrall G A 1985 Electrical breakdown in vacuum *IEEE Trans. Electr. Insul.* **20** 815–41
- [8] Guile A E and Hitchcock A H 1978 The erosion of copper cathodes from vacuum to atmospheric pressure arcs *J. Appl. Phys.* **49** 4275–6
- [9] Ding B, Yang Z and Wang X 1996 Influence of microstructure on dielectric strength of CuCr contact materials in vacuum *IEEE Trans. Compon. Packag. Manuf. Technol. A* **19** 76–81
- [10] Wang Y P and Ding B J 1999 The preparation and the properties of microcrystalline and nanocrystalline CuCr contact materials *IEEE Trans. Components Packaging Technol.* **22** 467–72
- [11] Wang Y, Zhang C, Zhang H, Ding B and Lu K 2003 Effect of the microstructure of electrode materials on arc cathode spot dynamics *J. Phys. D: Appl. Phys.* **36** 2649–54
- [12] Zhang C, Yang Z, Wang Y and Ding B 2003 Cathode spot propagation on the surface of amorphous, nanocrystalline and crystalline $\text{Cu}_{60}\text{Zr}_{28}\text{Ti}_{12}$ cathodes *Phys. Lett. A* **318** 435–9
- [13] Cobine J D and Gallagher C J 1948 Current density of the arc cathode spot *Phys. Rev.* **74** 1524–30
- [14] Juttner B, Pursch H and Shilo V A 1984 The influence of surface roughness and surface temperature on arc spots movement in vacuum *J. Phys. D: Appl. Phys.* **17** L31–4
- [15] Reece M P 1956 Arcs in vacuum *Nature* **177** 1089–90
- [16] Germer L H and Boyle W S 1955 Anode and cathode arcs *Nature* **176** 1019
- [17] Daalder J E 1974 Diameter and current density of single and multiple cathode discharges in vacuum *IEEE Trans. Power Appar. Syst.* **PAS-93** 1747–58
- [18] Daalder J E and Vos C W M 1972 Distribution functions of the spot diameter for single and multi cathode discharges in vacuum, Eindhoven University of Technology, Eindhoven, The Netherlands *Rep* 72-E-32
- [19] Fu Y H and Smeets R P P 1989 The influence of contact surface microstructure on vacuum arc stability and voltage *IEEE Trans. Plasma Sci.* **17** 727–9
- [20] Fu Y H 1989 The influence of cathode surface microstructure on DC vacuum arcs *J. Phys. D: Appl. Phys.* **22** 94–102
- [21] Lakshminarayana Rao, Munz R J and Meunier J-L 2007 Vacuum arc velocity and erosion rate measurements on nanostructured plasma and HVOF spray coatings *J. Phys. D: Appl. Phys.* **40** 4192–201
- [22] Plyutto A A, Ryzhkov V N and Kapin A T 1965 High speed plasma streams in vacuum arcs *Sov. Phys.—JETP* **20** 328–37
- [23] Kimblin C W 1974 Cathode spot erosion and ionization phenomena in the transition from vacuum to atmospheric pressure arc *J. Appl. Phys.* **45** 5235–44
- [24] Meunier J-L and Drouet M G 1987 Experimental study of the effect of gas pressure on arc cathode erosion and redeposition in He, Ar and SF_6 from vacuum to atmospheric pressure *IEEE Trans. Plasma Sci.* **PS-15** 515–19
- [25] Szente R N, Munz R J and Drouet M G 1992 Electrode erosion in plasma torches *Plasma Chem. Plasma Process.* **12** 327–43
- [26] Daalder J E 1975 Erosion and the origin of charged and neutral species in vacuum arcs *J. Phys. D: Appl. Phys.* **8** 1647–59